A PRELIMINARY REPORT ON THE TERRAIN ANALYSIS OF THE LUNAR EQUATORIAL BELT

by

John F. McCauley

July 1964

This report concerns work done on behalf of the National Aeronautics and Space Administration.

This report is preliminary and has not been edited or reviewed for conformity with U. S. Geological Survey standards and nomenclature.

CONTENTS

	Page
INTRODUCTION	1
DISCUSSION OF TECHNIQUES	3
Photometric slope measurements	3
Shadow variation measurements	12
Visual studies	14
High resolution photography	17
Terrestrial slope frequency distribution studies	17
RESULTS	19
Slope frequency distribution as a means of classifying terrain	19
A quantitative classification of lunar terrain	27
Terrain classification map of the lunar equatorial belt	31
Integrated slope distribution map	33
Visual studies	35
Terrestrial slope frequency distribution studies	37
Extrapolation of roughness below the limit of resolution	42
REFERENCES	44

INTRODUCTION

The U. S. Geological Survey began, in November 1963, a terrain analysis of the lunar equatorial belt (10°N-10°S, 60°W-15°E), on behalf of the National Aeronautics and Space Administration. The purpose of the study is to establish a quantitative classification system in terms of different degrees of relative resolvable roughness, using the best available earth based techniques, the resolution of which averages one kilometer. Those parts of the lunar surface that have the least resolvable roughness at this scale have the highest statistical probability of containing safe landing areas at the one to ten meter scale for both manned and unmanned spacecraft.

This preliminary report is based on eight months work prior to July 1, 1964: an unreviewed manuscript was submitted initially to the National Aeronautics and Space Administration on July 27, 1964. The report does not include any data derived from Ranger VII, and manuscript review subsequent to Ranger VII has not revealed the need for any significant changes in the conclusions.

The major results are: 1) a quantitative terrain classification of the equatorial belt, chiefly in the form of a map (Plate 1), but including slope frequency distribution curves for each unit; 2) four larger scale maps (1:1, 000, 000) of the central part of the belt showing the areal distribution pattern of approximately 30, 000 individual slope measurements; 3) a large scale terrain map of the Flamsteed area, studied visually at the Lick 36" refractor, to determine the relative surface roughness below the limit of photographic resolution: 4) a full discussion of all the major techniques employed in the study

i. e., photometric slope measurement, slope measurement by shadow variation, high resolution photography, and visual study techniques; 5) an extrapolation of derived roughness information below the limit of photographic resolution. The extrapolation is based primarily on the behavior of the lunar slope data through a wide range of resolution and on information derived from studies of different terrestrial areas at varying degrees of resolution.

DISCUSSION OF TECHNIQUES

Photometric Slope Measurements

The most important technique used in this study from the standpoint of quantitative data for terrain classification was a photometric slope measuring method. It employs the best available high resolution lunar photography and is capable of accurate measurement in the east-west direction for elements of the lunar surface as small as three-quarters of a square kilometer in size. This general technique was first employed by van Diggelen (1951), in a study of mare ridges, and was subsequently applied by Dale (1962) to a more general study of the topography of the maria. Wilhelms (1963) refined the technique and first applied it successfully to other types of lunar terrain. Experimental work for the purpose of developing mapping applications with the imaging systems of unmanned spacecraft has been described recently by Amdursky, Marsh, and Graboske (1964). The present study has led to further development of the method employing automatic scanning techniques with computer analysis so that thousands of individual slope measurements can be readily generated.

The technique is primarily based on the observation that the brightness of an element of the lunar surface is a function of the normal albedo, the slope of the surface and the sun's angle of elevation. Normal albedo is here defined as the fraction of the incident light reflected to the earth from the lunar surface at full moon illumination. If the effect of variation of normal albedo from point to point on the lunar surface can be eliminated, the brightness of an element of the surface would then depend only on slope and

the sun's angle of elevation which can be expressed in terms of differences in lunar longitude near the equator.

This relationship can be seen in Figure 1, which represents a polar view of the Moon, on which the surface elements P and Q have the same albedo, and also have the same brightness because of their similar angular relationship to the sun. Angles COQ and CPD are equal; but CPD equals angle AEB, the E-W component of slope for element P. This angle AEB (E-W slope component) can be expressed in terms of the difference in lunar longitude between elements P and Q, or the difference in the sun's angle of elevation for measurements made near the equator. Therefore, if two surface elements, separated in the E-W direction, have the same albedo and the same measured brightness, the slope of the inclined element is equal to the difference in lunar longitude or difference in angle of sun elevation between them. If the relative albedo of different parts of the lunar surface can be determined, and if the brightness of the horizontal areas is determined as a function of lunar longitude, then the E-W slope components can be readily determined.

Essential to the technique is the ability to discriminate differences in normal albedo within the sample area. The most effective method tested proved to be a modification of that first described by Hawkins and Munsey (1963) for an entirely different application. It involves exposing a high resolution full moon photograph (Lick Observatory, January 17, 1946) to a very high contrast photographic material (Kodak, Ortho Litho S) in a series of graduated exposures. At each graduated exposure step, the

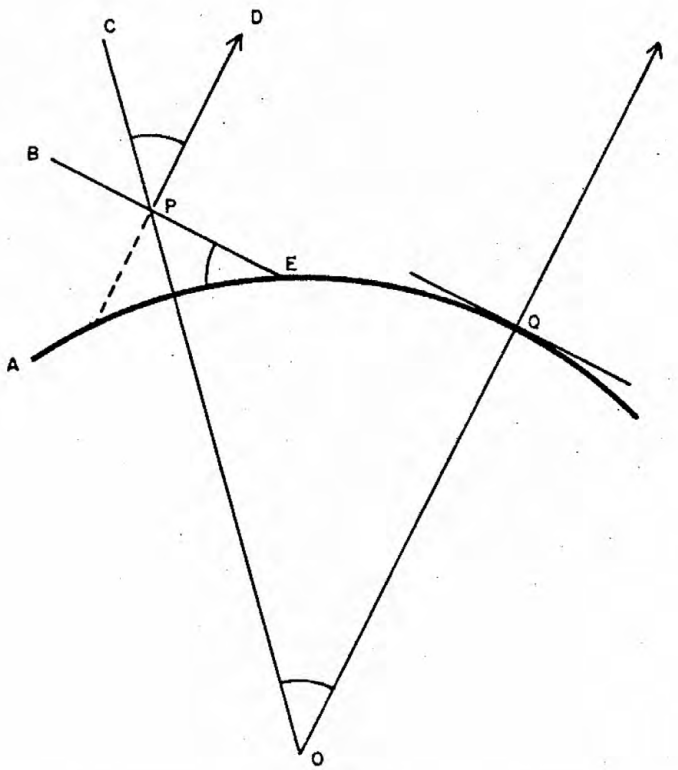

Figure 1. The relationship between brightness and slope on the lunar surface.

photographic response was either black or white, thereby giving the areal distribution pattern of relative normal albedo for each particular exposure. By superimposition of the series of black and white images derived, it was possible to prepare an isopleth map showing the distribution of six albedo units (Figure 2). Information on these changes in relative albedo are introduced into the computer

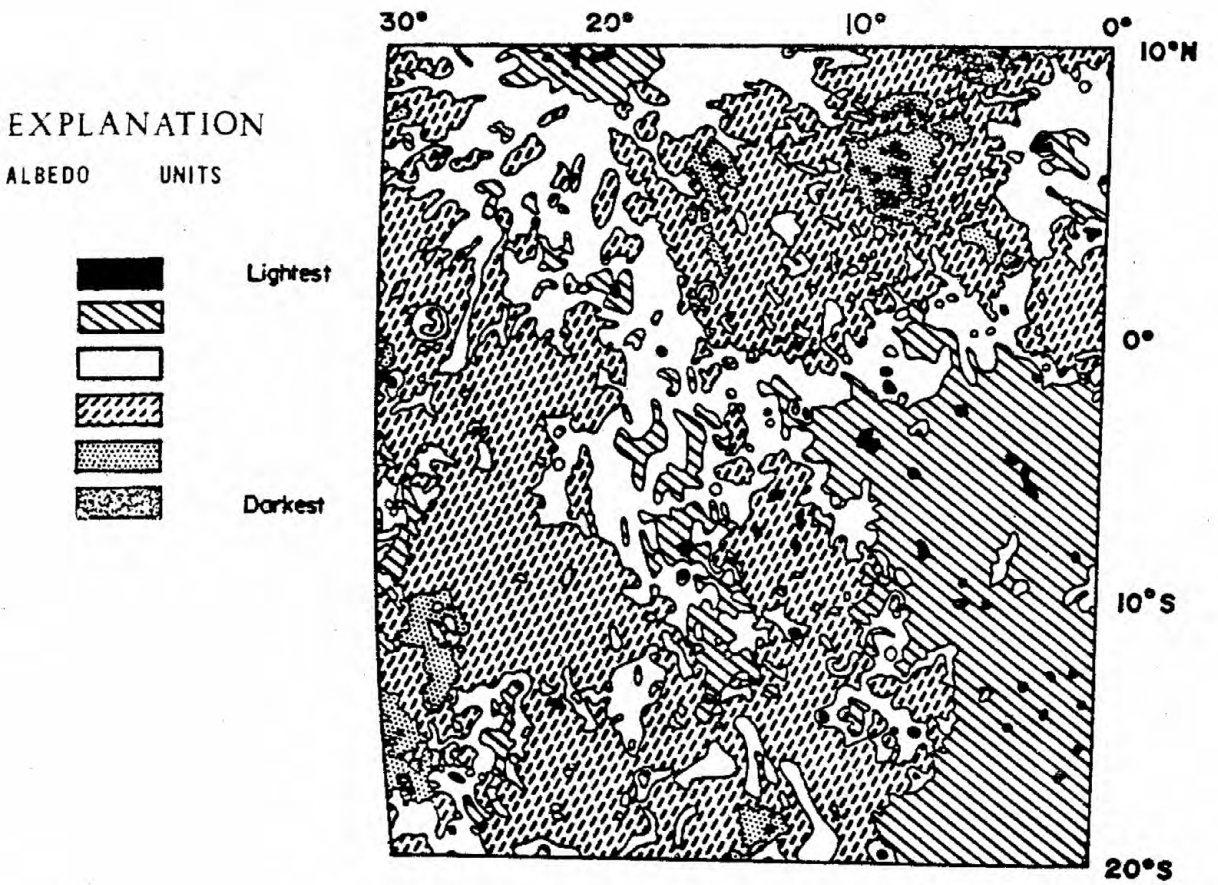

Figure 2. Isopleth map showing the distribution of six normal albedo units derived by the "black-white" photographic technique.

program by the microphotometer operator at the time the plate being used for slope measurement is scanned. In this way, different plate intensity measurements can be equated directly with surface topographic irregularities or slope, and the effect of lateral gradation in albedo is eliminated.

The variation of plate brightness with lunar longitude or sun elevation independent of slope must be determined for each relative

albedo unit on the plate. This is accomplished by measuring the brightness of areas with little or no resolvable relief at different longitudes within each albedo unit and plotting these points as a function of distance in lunar longitude from the terminator. A "least squares fit" is then made to derive a curve that represents the variation of plate brightness as a function of sun elevation independent of the effect of local slope. The curve so derived is referred to here as the "standard curve" for the respective albedo unit, and it effectively represents the results of the lunar photometric function, the plate response, and the response of the microphotometer. Departures in brightness from these curves measured during a plate traverse are the result of local slope in an east-west direction. Figure 3 exhibits how an individual reading "X" within relative albedo unit 3 is compared with a point of equal brightness "Y" on the standard curve to determine the slope of "X" which is 2. 2 degrees. Large changes such as those seen between points A and B, and C and D are typically the result of albedo differences encountered during a plate traverse whereas changes like those between E, F, and G are generally the result of topographic irregularities on the lunar surface. Individual brightness readings are referred by the computer to their appropriate "standard curve" for slope determination by means of commands introduced during the plate traverse by the microphotometer operator.

The measurements are made with a Jarrell-Ash 100, recording microphotometer, the stage of which has been modified to permit automatic scanning of a negative plate at a fixed rate

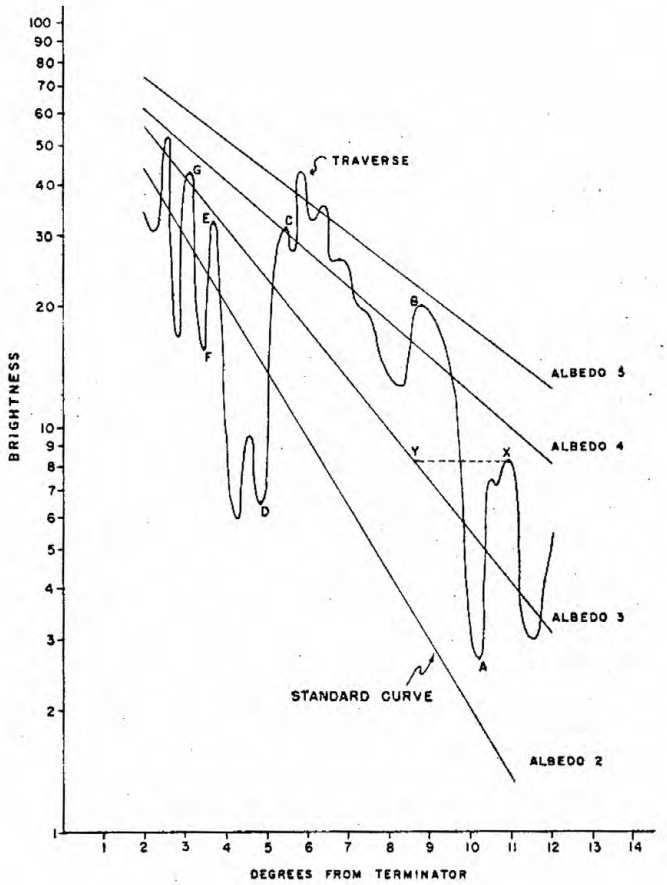

Figure 3. Idealized photometer traverse on the lunar surface, and the "standard curves" for different relative albedo units for a particular lunar plate. The effects of both albedo and local slope are seen on the traverse.

in any direction. It has been found more convenient to use negative rather than positive lunar plates because of the response characteristics of this machine. The traverses are made in an east-west direction over a relatively small part of the plate, two degrees to 12 degrees from the terminator, where the lunar photometric function is most sensitive to the effects of local slope and the sensitivity of the microphotometer is greatest.

Areas as small as three-quarters of a square kilometer of the lunar surface can be sampled when employing high resolution plates. The brightness values for these areas are digitized, then punched out on paper tape for computer processing. In practice, alternate three-quarter square kilometer segments are actually sampled because of the limitations of the digitizing equipment used with the microphotometer.

In a typical ten degree wide traverse (two degrees to 12 degrees from the terminator), approximately 200 individual slope readings are obtained. The traverses in these preliminary studies, were spaced approximately five to ten kilometers apart. Therefore, approximately 12, 000 individual slope readings in a north-south direction are obtained from a single plate representing ten degrees of lunar longitude and 20 degrees of latitude. The current study has generated approximately 40, 000 individual slope measurements within the equatorial belt.

The photometric technique is most effective in areas of low slope, that is, slopes generally less than five degrees. The reason for this limitation is that black shadows are present on the plate when the average slope at a particular point is greater than the sun's angle of elevation (number of degrees of lunar longitude between the sampled point and the terminator). Areas consisting of rough terrain and high average slope values

contain a preponderance of shadow near the terminator and their roughness must be measured by other techniques.

Since the photometric slope measuring technique, as applied here, is limited to zones of only ten degrees in an east-west direction a considerable number of overlapping high resolution photographs are necessary to cover the specified area within the equatorial belt. The very best currently available high resolution lunar photographs are those of the Lick-Herbig Series taken with the 120" reflecting telescope. Unfortunately, the majority of these lie outside the equatorial belt and none were employed in this study. The next best series of photographs from the standpoint of resolution are the Mt. Wilson-Pease Series taken at the 100" reflector which, although of considerable age, do provide a sufficient variety of terminator positions to assure reasonable coverage of the equatorial belt. Many of the plates in this series, however, proved upon initial photometric scanning to have uneven exposures; these were rejected and only photometrically uniform plates of the highest available resolution employed. A list of the five plates used during this study is given in Table 1. Although individual photographs from other observatories may be superior for certain parts of the equatorial belt, the decision to use the Mt. Wilson plates exclusively was prompted by a desire to avoid plate reproduction and scale problems which would have greatly complicated the automatic sampling program.

Table 1. List of plates used for photometric slope measurements.

Plate	Date	Time	Terminator
Pease 111	9-14-19	12:58 UT	30.3° E
Pease 124	9-15-19	15:44 UT	7.7° E
Pease 192	10-4-20	12:20 UT	5.1° W
Pease 252	9-24-21	11:00 UT	12.15° W
Pease 172	7-9-20	11:44 UT	12.60° W

This photometric slope measuring technique provides data only in the east-west direction, and the measurements represent slope components in this direction rather than true slope. All profile measuring techniques, however, are similarly limited to slope component measurements except where the slopes are unidirectional and measurements are made at right angles to the slope direction. If the measurements are made at any other angle, it is necessary to correct for true slope which is always the greater value. Corrections to the slope component measurements can also be readily made in cases of random slope orientation. It has not been necessary to apply corrections to measured slope components in this study, since the relative order to terrain roughness is unaffected by this computation. The average slope values given, however, should be considered minimal estimates of the actual slope distributions.

Shadow Variation Measurements

Since the photometric slope measuring technique is effective only in areas of relatively low slope, quantitative information on the rougher parts of the lunar surface must be obtained by an independent method. The shadow variation technique first described by Pohn, Murray, and Brown (1962) is applicable to this problem. It is based on the fact that the area in shadow on the moon at any particular time is a function of the local relief and the sun's elevation. For a shadow to be present on the illuminated part of the moon, a local topographic element must have an average slope greater than the sun angle elevation at that point. A series of photographs of the same area with differing sun elevation angles can be used to measure the percent area in shadow at each different sun elevation to provide a minimal estimate of the slope frequency distribution (Figure 4).

In actual practice the photographs are arranged in order of decreasing sun altitude, and a photograph with a sun elevation of between eight degrees and 12 degrees selected for initial measurement. The reason for this is that at higher sun altitudes the shadows cast appear to be gray because of the presence of partially illuminated unresolved features within the shaded areas. At lower sun altitudes, the effects of penumbral shadow are great, and it is difficult to measure the shadowed areas accurately.

The shadowed area on the eight to 12 degree angle photograph is carefully traced and the percent shaded area determined. Particular

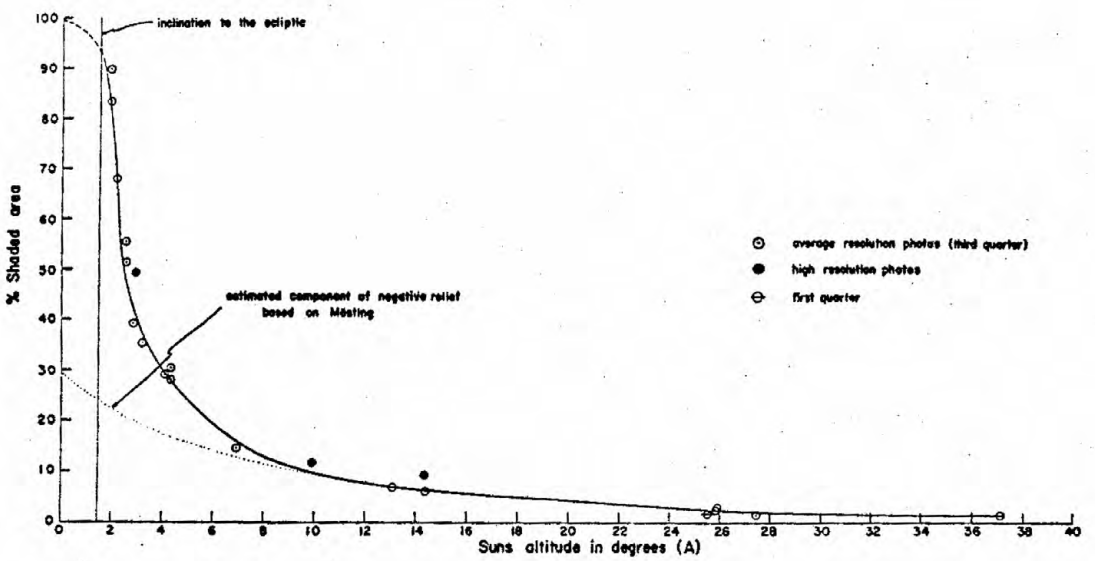

Figure 4. Shadow variation curve for the Argelander area (after Pohn, Murray, and Brown, 1962).

success has been obtained from a modification of the point counting method used in microscopy (Chayes, 1956). It has the advantage of being simple, rapid, and reproducible to within $\pm$0. 5 percent. After the first photograph is completed, one can work with photographs of higher and lower sun angles.

The total percent of shadowed area for each photograph was plotted as a function of the sun elevation or the minimum

slope angle (Figure 4). The diagram derived is similar to the cumulative frequency diagrams used to present photometrically derived slope information. However, it is more effective in rough areas and therefore, compliments the other technique. Both methods have been used to develop the quantitative terrain classification of the equatorial belt presented later in this report.

Visual Studies

It is well established that one is able to resolve details at the telescope visually that cannot be captured on photographic emulsion. In order to study the fine structure of the lunar surface it is necessary to observe small areas systematically with telescopes of large aperture and high resolving power. Atmospheric seeing conditions are the most significant limitation to visual studies, and the derivation of detailed surface roughness information requires relatively rare interludes of excellent "seeing".

One of the most effective visual telescopes in existence is the 36" refracting telescope at Lick Observatory. This instrument has been used extensively in the terrain analysis program along with the 60" McMath telescope at Kitt Peak, Arizona. Eight areas (Table 2) within the equatorial belt were selected initially for detailed visual study. The criteria used in selecting

these areas were essentially fourfold:

1. Apparent smoothness on the best existing earth-based photographs;
2. relative smoothness on the basis of photometric slope measurements;
3. remoteness from relatively recent large craters;
4. freedom from both linear and diffuse rays which previous work has shown to be very rough at the limit of resolution.

Table 2

Area	Location	Observer
1	1°S - 4° N Lat 3° E - 3° W Long	Masursky
2	2° S - 2° N Lat 10° W - 16° W Long	Hose
3	2° S - 10° S Lat 9° W - 15° W Long	Irwin
4	6° S - 10° S Lat 19° W - 28° W Long	Bailey
5	0° - 6° S Lat 30° W - 38° W Long	Moore
6	2° S - 4° S Lat 42° W - 46° W Long	Crowder
7	7° S - 9° S Lat 48° W - 53° W Long	Crowder
8	1° S - 5° S Lat 58° W - 60° W Long	McCauley

Emphasis is on the plotting of the smallest craters that can be resolved under conditions of excellent seeing. This will provide fundamental information on the crater density at the limit of resolution, and thereby permit more accurate extrapolation of crater frequency distributions to the scale of interest for landing spacecraft. Other small scale relief features, such as ridges, rilles, and local topographic irregularities are also plotted. In addition, estimates of the relative resolvable roughness from place to place can be made that are more accurate than those derived photometrically.

During the period covered by this report (November 1963 - July 1964), the eight study areas were observed a total of approximately 50 nights with an average observing period of two to three hours. Unusually bad atmospheric conditions, however, were experienced during this interval at Lick Observatory, California, at Kitt Peak Observatory, Tucson, Arizona, and at Flagstaff, Arizona. Only one of the assigned observers experienced "seeing" of sufficiently high quality to perform detailed mapping. A preliminary map (Figure 10) at a scale of 1:1, 000, 000 showing the relative roughness within the area is included in this report.

High Resolution Photography

The Astrometric camera for the Lick 36" refracting telescope has been modified according to specifications provided by the U. S. Geological Survey to yield a range of possible exposures from 1/300 of a second up to six seconds. The camera will be available to the observers studying areas visually to provide a means of documenting their observations at low angles of illumination and to provide additional high resolution photographic plates from which slope information can be acquired photometrically. Preliminary experiments with the camera system under conditions of poor "seeing" have provided several new full moon photographs of good quality. It is expected that an extensive collection of high quality lunar photographs will be acquired with this telescope during the 1965 Fiscal Year.

Terrestrial Slope Frequency Distribution Studies

A study of different types of terrestrial terrain at varying scales was undertaken in order to provide the basis for a better understanding of quantitative terrain classification and to test the reliability of extrapolating roughness from one scale to another as the size or "resolution" of the sample is changed.

The base materials used for this study include USAF Operational Navigation Charts at a scale of 1:1, 000, 000, which

approximate in scale and contour interval, the Lunar Aeronautical Charts published by the Aeronautical Chart and Information Center, U. S. Air Force. In order to determine the effect of increasing resolution on the roughness of a terrain unit, the same general areas were studied at scales of 1:250, 000 and 1:62, 500 using maps published by the U. S. Geological Survey.

The areas selected represent three distinct geomorphic provinces: the Sierra Nevada Region, California; the San Juan Mountain Region, Colorado; and the Mogollon Rim Region, Arizona. Each area was studied at the 1:1, 000, 000 and 1:250, 000 scale, and the Sierra Nevada Region was also studied at 1:62, 500. However, instead of deriving slope information by the photometric technique, the slopes were derived from a series of topographic profiles, on which slopes for alternate segments of varying size were measured. The slope lengths ranged from approximately one kilometer to a tenth of a kilometer in size for the largest scale map. This represents a fairly accurate simulation of the photometric slope measuring technique but is not restricted to measurements of low slope angles, i. e., less than 12 degrees. Therefore, the slope frequency distributions derived proved to be generally normal, whereas those derived photometrically are skewed in the direction of lower average slopes.

RESULTS

Slope Frequency Distribution As a Means of Classifying Terrain

Slope is the principal determinant of surface geometry and can be used as a means of expressing terrain roughness at any selected scale if a sufficient number of slope readings are available for classification purposes. One type of slope classification found to be very effective is the cumulative frequency diagram that not only expresses the percentage of area in terms of various slope categories but also provides information on the range or dispersion of slope values about the average. This diagram has been used in this study to express statistically the relative roughness of lunar terrain. The most effective parameters derived from this statistical approach are the median (50 percentile value) which is the most easily derived measure of central tendency, and which generally can be used directly to express relative average roughness for a particular area. The 10-90 percentile range is an effective measure of slope value dispersion and can be considered as an expression of the variability of terrain. The mode is also useful in describing terrain roughness since it gives the slope value that occurs most frequently within the sample area. The standard deviation, which is a measure of the degree of dispersion of the slope values about the mean can also be considered an index of variability but it appears less efficient for this purpose than the 10-90 percentile range, (Table 3).

The median slope values, the modes, and the arithmetic means for slope populations derived photometrically do not generally coincide because of the tendency of this method to over-emphasize low slope readings. The divergence between the modes and the means is particularly evident in rougher terrain where the majority of the distributions are right skewed, i. e., the value of the mean is greater than the value of the mode. The average slope values given for classification purposes must then be considered minimal estimates.

Table 3 represents a statistical summary of slope data from 12 separate areas within the equatorial belt considered typical of the range of different types of lunar terrain at the limit of telescopic resolution. Figure 5 shows slope frequency curves for several typical areas clearly indicating the behavior of the median and the 10-90 percentile dispersion in smooth, intermediate and rough terrain. Figure 6 gives the location of the sampled areas within the equatorial belt. Sampled areas one through four are the smoothest and consist of different areas within the maria. The median slope value for these areas ranges from 0. 95 degrees to 1. 30 degrees, and the 10-90 percentile range is from 1. 50 degrees to 2. 00 degrees. Sample 1, in the northern part of Mare Nubium, is free of nearby large craters, rays, mare ridges, and domes, and appears at the limit of photographic resolution to be the smoothest large area within the equatorial belt. The Sinus Medii area, sample 2, contains several medium size craters, such as Bruce and Blagg, along with numerous mare ridges, and is, therefore, measurably rougher than those parts of the maria free of resolvable craters.

TABLE 3

Sample	Median	Mean	Mode	Std Dev	Dispersion	Population	Description
1	0. 95	0. 93	00. 0-0. 49	0. 20	1. 50	440	Mare, between Parry B & Davy K.
2	1. 10	0. 94	0. 50-0. 99	0. 67	2. 00	658	Mare in Sinus Medii between Pallas D and Rhaeticus L.
3	1. 25	1. 19	0. 50-0. 99	0. 87	2. 00	357	Mare between Gambert K & Gambert G.
4	1. 30	1. 50	1. 00-1. 49	1. 59	2. 00	440	Mare in Sinus Aestuum between Stadius C and Shröter C.
5	1. 95	1. 43	0. 50-0. 99	1. 22	3. 00	111	Mare domes north of Hortensius.
6	1. 43	1. 50	0. 00-0. 49	1. 48	2. 50	265	Floor of upland crater Flammarion.
7	1. 42	1. 60	1. 00-0. 49	1. 06	2. 50	62	Central part of loor of upland crater Fra Mauro.
8	2. 65	2. 46	2. 00-2. 49	2. 71	3. 00	333	Floor of upland crater Ptolemaeus.
9	2. 20	2. 60	00. 0-0. 49	2. 50	4. 00	345	Smooth regional material between Hyginus C and Silberschlag contains several major rilles.
10	1. 98	2. 21	00. 0-0. 49	2. 49	4. 00	459	Southern part of rim of crater Copericus between Copernicus E and Fauth F.
11	2. 37	2. 59	00. 0-0. 49	2. 30	5. 50	394	Eastern part of rim of crater Copernicus between Copernicus E and Fauth G.
12	4. 30	4. 61	1. 50-1. 99	3. 30	8. 00	740	Cratered upland surrounding the crater Herschel.
						4604	

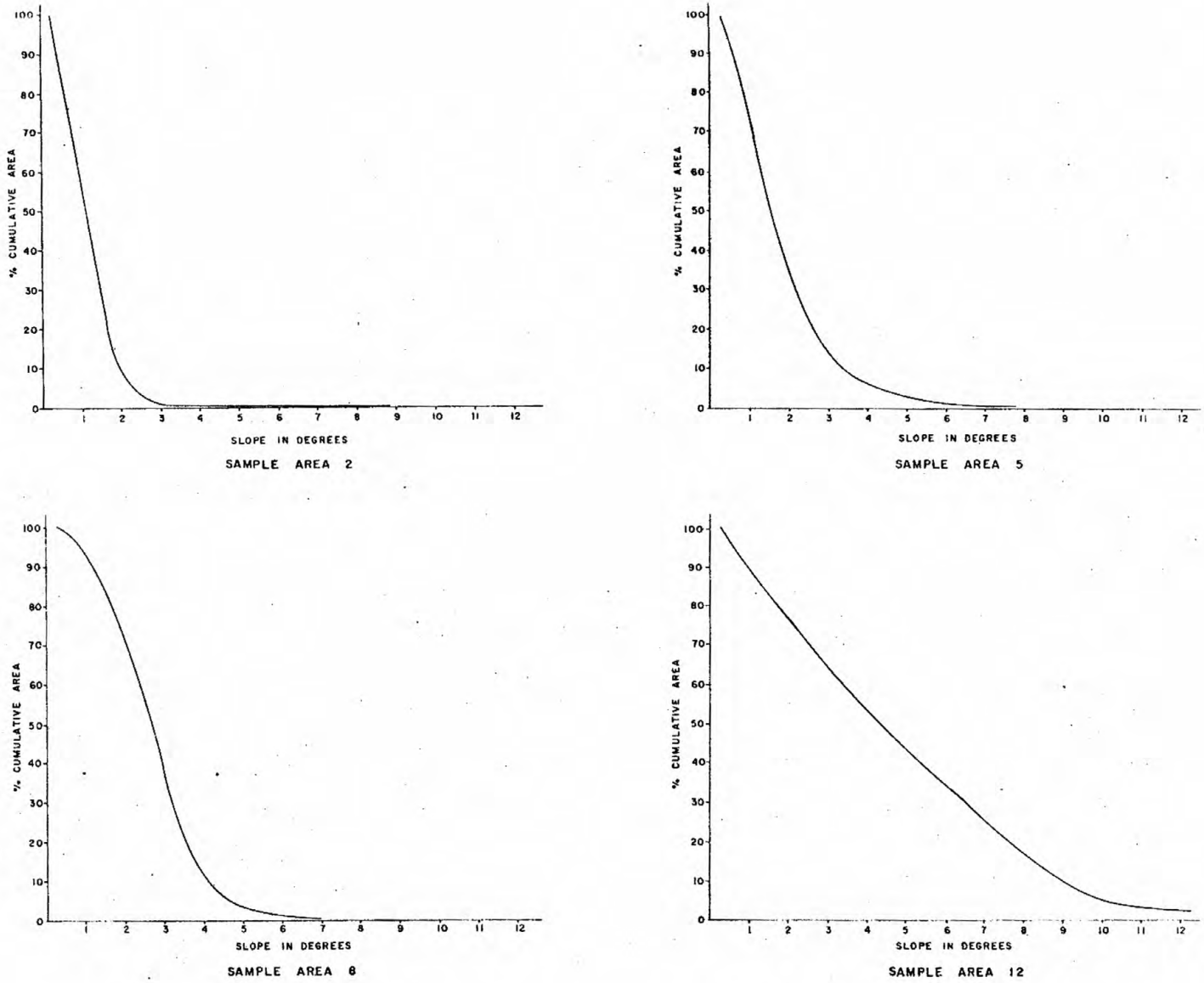

Figure 5. Typical slope frequency distribution curves for selected parts of the lunar surface. Areas correspond to those described in Table 3.

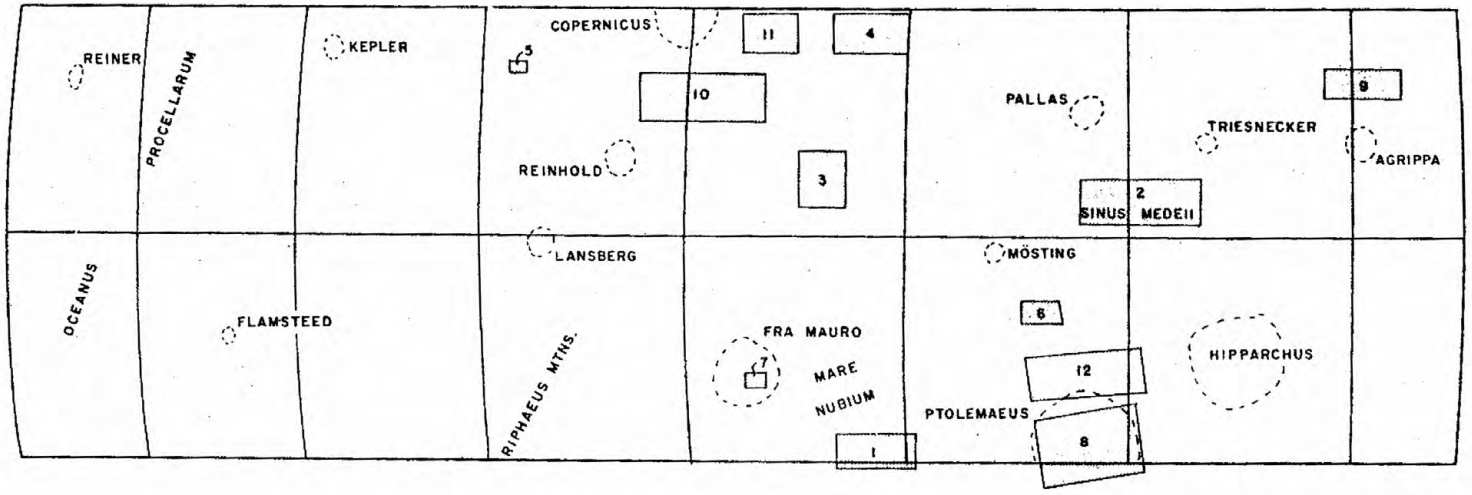

Figure 6. Location map for the different lunar terrain areas described in Table 3.

Sample 3, northeast of Gambert, contains several mare ridges, and is close to the large craters Gambert B and C, but its observed roughness is only slightly greater than that of Sinus Medii. Sample 4, at the southern end of Sinus Aestuum, contains a number of mare ridges, but its greater roughness is attributed primarily to the presence of numerous small secondary craters derived from both Copernicus and Eratosthenes. Sample 5 consists exclusively of the cluster of small domes north of the crater Hortensius which are significantly rougher than the average maria at the limit of photographic resolution. Visual studies indicate that, in addition to being characterized by one to two degree regional slopes, the surface of these domes is clearly rougher than the surrounding terrain.

The values for the mode and the arithmetic mean for these five units are reasonably close and the statistical slope distributions are, therefore, approximately normal. In the case of normal distributions both the median or the arithmetic mean slope can be used as effective indicators of relative roughness if combined with a measure of dispersion such as the 10-90 percentile value or the standard deviation both of which increase as the roughness or non-uniformity of the terrain increases.

Samples 6 through 8 consist of the floors of the large upland craters Flammarion, Fra Mauro, and Ptolemaeus. The Flammarion and Fra Mauro areas are considerably rougher than average mare, but actually smoother than the mare domes near Hortensius. Ptolemaeus is clearly the roughest of these three upland crater units, probably as a result of the presence of

numerous ghost craters beneath a blanket of smoother surficial regional material.

Sample 9 consists mostly of lunar terrae or upland exhibiting numerous structural features such as rilles and small chain craters which contribute significantly to the average roughness.

Samples 10 and 11 are two different sample areas adjacent to the crater Copernicus. The sample on the southern rim is generally further from the center of the crater, and the resolvable relief here results in great part from the presence of numerous irregular secondary craters derived from the Copernicus and superimposed on the surrounding maria. The eastern rim sample is closer to the center of the crater, and its measurably greater relief results primarily from the hummocky terrain typical of the inner rims of large lunar craters. These two samples are considered a reliable index to the character of the rim terrain surrounding all major relatively recent lunar craters. Rim deposits are, therefore, considered to represent some of the roughest terrain sampled. The total roughness or slope distribution of the entire crater unit, that is, the central depression, and the associated rim deposit, cannot generally be measured by the photometric technique since the interior slopes are mostly in shadow. The shadow variation technique of Pohn et al. (1962) however, has been used to supplement the photometric information for the purpose of determining the average roughness of the entire crater unit. Figure 7 expresses the relationship between percent shaded area of the interior of the crater as a function of the angle of sun elevation. It, therefore, is a measure of the minimal topographic roughness within the crater.

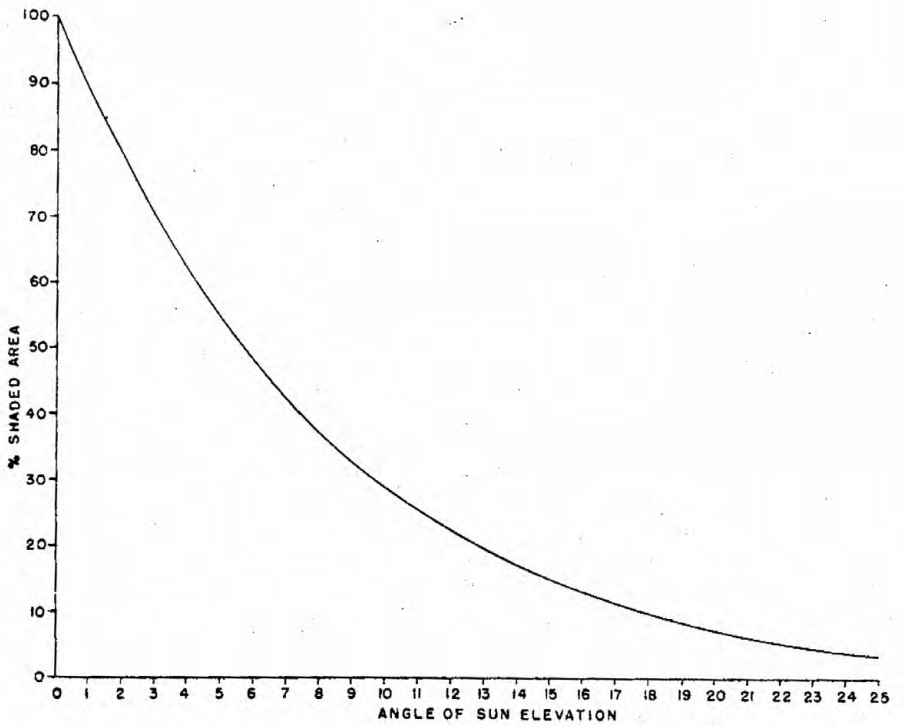

Figure 7. Shadow variation curve for Copernicus (interior walls and floor) (by Pohn).

The median slope value here is 5. 8 degrees, and the 10-90 percentile range is 18 degrees. By comparison with the data in Table 2, it can be seen that a young crater of the Copernicus type (rim deposit and interior slopes) does represent, in its entirety, very rough terrain. Comparison of the numerical roughness parameters with certain types of terrestrial surfaces, later in the report, will serve to emphasize this point.

Sample 12 represents a part of the very rough cratered upland near Herschel, typical of the terrae within the equatorial belt. These are clearly the roughest parts of the Moon investigated, as indicated both by photometric slope measurements, as well as by those of the shadow variation technique. Figure 8 gives the shadow variation

curve for this terrain south and west of the crater Flammarion. The median is 3. 5 degrees and the 10-90 percentile range is ten degrees, both parameters indicating a very rough surface at the current limit of resolution.

A Quantitative Classification of Lunar Terrain

A primarily quantitative classification of lunar terrain applicable at the one kilometer scale has been derived from the 40, 000 individual photometric slope measurements made within the equatorial belt. Where necessary, data derived from shadow progression studies and visual telescopic observations have been applied. This classification provides the basis for mapping the areal distribution of relative roughness on the lunar surface.

Six fundamentally distinct topographic units are recognized at this time and designated Terrain Units I - VI. Cumulative slope frequency diagrams for each unit are given in Figure 9.

Unit I: The median slope within this unit ranges from zero in small areas of no resolvable relief to approximately 1. 5 degrees. Measured slope values show a narrow range, and the statistical distributions derived are generally normal. Physiographically, the terrain generally consists of the darker parts of the maria, away from large, relatively recent craters, and devoid of structures such as ridges, domes and rilles. Samples 1 and 2 in Table 3 are typical examples.

Unit II: Quantitatively, this unit is identical to Unit I. It consists of the lighter ray covered parts of the maria, and can be distinguished from Unit I by its higher albedo. Visual studies below the limit of photographic resolution indicate that these areas are

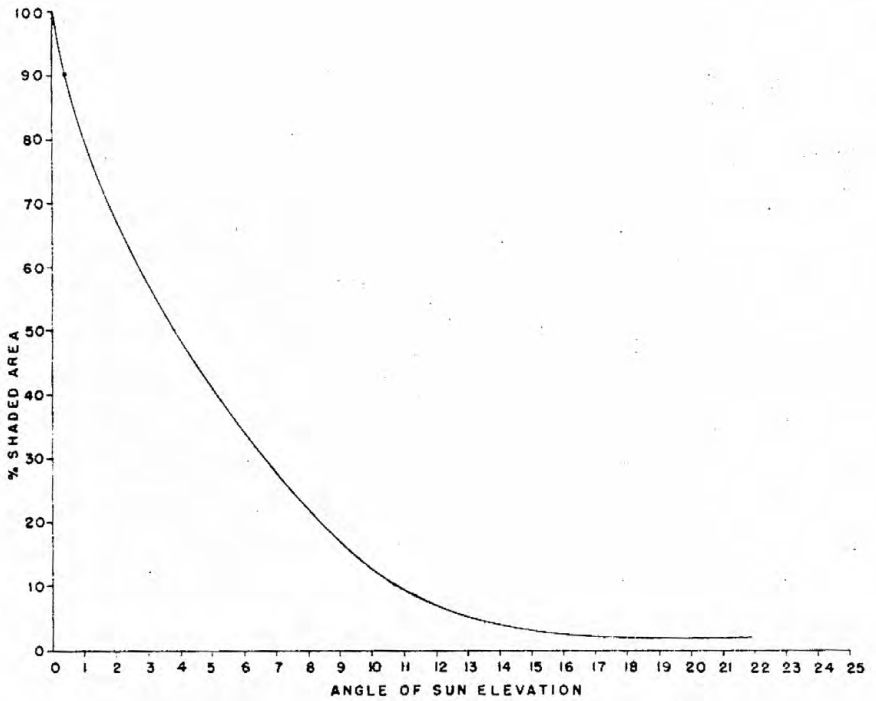

Figure 8. Shadow variation curve for the Flammarion area.

rougher than the darker parts of the maria primarily because of the presence of numerous very small secondary craters at or just below the limit of recognition.

Unit III: Median slope ranges from one degree to two degrees in this unit, with the typical example at 1. 5 degrees. Physiographically, the unit consists of mare areas containing numerous structural features such as mare ridges, rilles, and domes. Some of the smooth regional material in the uplands or terrae, however, shows the same degree of quantitative roughness. A good example of the first type of terrain within this unit is Sample 5, Table 2.

Unit IV: The median slope value lies between 1. 5 to 2. 5 degrees and a 10-90 percentile range is three to four degrees. These areas

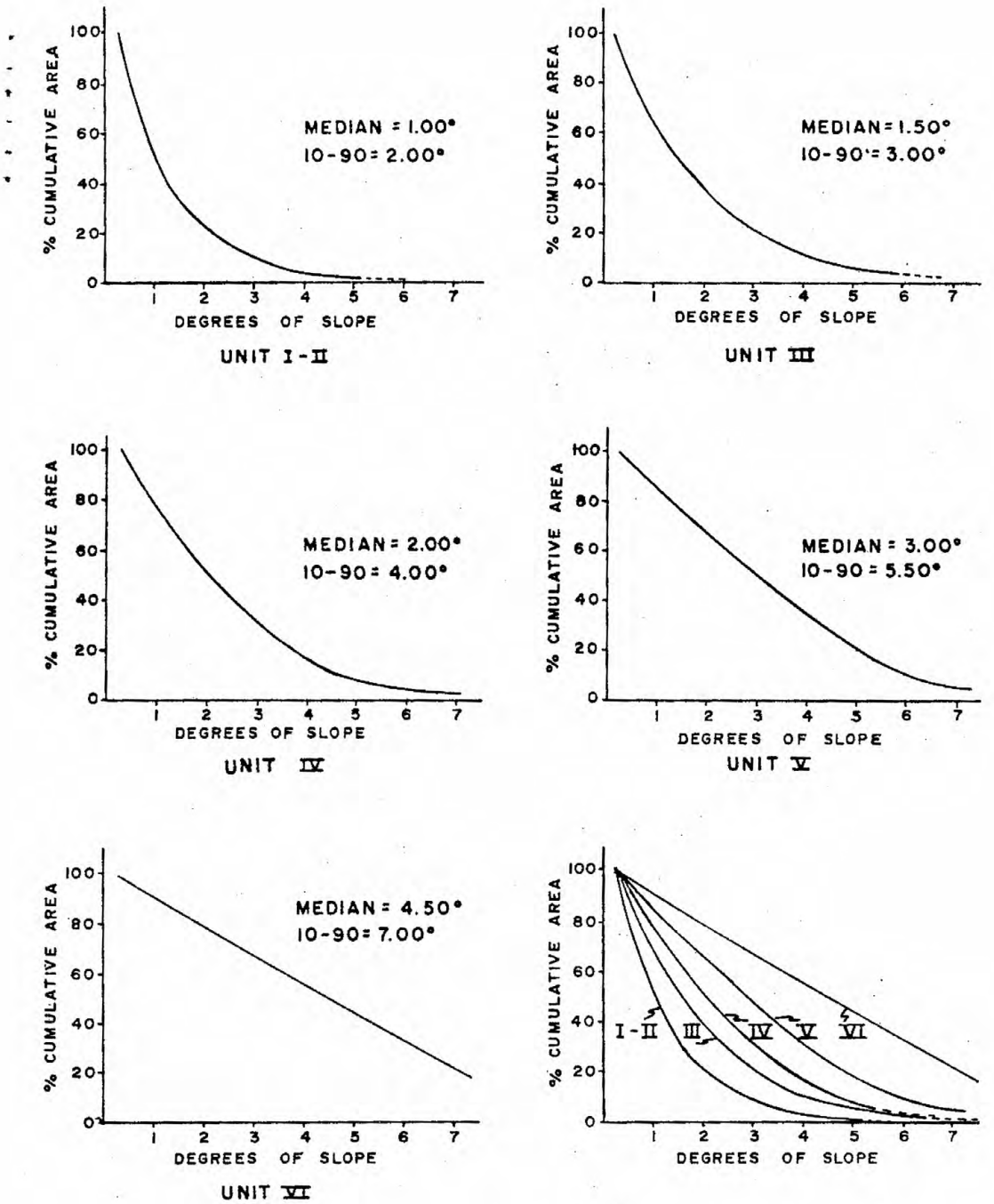

Figure 9. Slope frequency distribution curves for the idealized terrain units (I through VI) used in the classification of the equatorial belt.

consist of basins representing the floors of very large craters within the highlands. Sample 7, Fra Mauro, and Sample 8, Ptolemaeus, Table 3, are good examples. The frequency distributions within this unit are generally normal, and the range of absolute slope values are relatively small, as indicated by shadow progression studies.

Unit V: Median slope frequency, as determined both from photometric measurements and from shadow progression studies, ranges from two to six degrees. It consists of individual craters and their rim deposits (for a distance of approximately one crater radius). The roughness of these units is generally greatest along interior crater walls, which have average slopes of 37 degrees.

Unit VI: Median slope frequency, as determined both by photometric measurements and shadow variation studies, ranges from three degrees to a maximum of about eight degrees. These areas are characterized by a complex overlapping network of craters of various ages along with intercalated regional material, presumably derived from the major lunar basins, i. e., Imbrium, Humorum, etc. The photometrically derived slope distributions for this terrain show an excess of low slope values and a relatively narrow range of values and, therefore, represent very minimal estimates of the actual resolvable roughness. The shadow variation measurements give higher median values, and also show greater ranges or dispersion around the median. These measurements are considered more indicative of the real slope distribution at the one kilometer scale.

Terrain Classification Map of the Lunar Equatorial Belt

The terrain classification previously described has been applied within the equatorial belt (10°N - 10°S, 60°E - 15°W), and is shown in Plate I. This map was compiled from photometric measurements made during this study, and from published and unpublished geological maps of the equatorial belt. The majority of the systematic photometric measurements were made within 20 degrees of the prime meridian (0° longitude) because of the availability of good photography in this region. The remainder of the belt, because of the time limitations of the project and lack of suitable photography was sampled locally to establish and check correlations between units.

A serious problem concerning this map, and one affecting all studies of the lunar surface, either photometric, photographic, or visual, is foreshortening toward the limb regions. The resolution for all slope measuring methods falls off with cosine of the angular position from the prime meridian. At 60 degrees from the center of the moon the resolution is about one half that available in the central part of the disk. It is apparent from Plate 1 that the majority of the largest smooth areas (Terrain Unit I) are in the western part of the equatorial belt beyond 30 degrees west longitude. This can be attributed, in part, to regional considerations, because this is the location of the broad and relatively featureless Oceanus Procellarum. However, the high density of apparently smooth mare areas in this region is also the result of the inability of the photographic plate to

capture the fine structural details which are readily detected toward the center of the moon. Therefore, the map must be interpreted with caution beyond 30 degrees from the mean liberation point of the moon.

The main purpose of Plate 1 is to separate those areas which have a greater probability of containing smooth areas at the one to ten meter scale from those which are likely to contain very few suitable spacecraft landing sites. In order to do this the lunar surface has been classified into different terrain units in order of increasing roughness as previously described, and the areal distribution of these plotted. The units however, express relative quantitative roughness at the one kilometer scale which might be considered too small to have any bearing on the problem of spacecraft landing sites. Studies of the relationship between roughness and resolution to be discussed fully in a later section of this report indicate that the median slope value, and the slope dispersion for both lunar and terrestrial terrain increases with increasing resolution. In other words, roughness is additive with increasing resolution; the rate of increase generally being greater for rough terrain at the one kilometer scale than for smooth areas (Figure 11). Therefore, if terrain can be arranged in order of relative roughness at the one kilometer scale, this relative order will remain constant with increasing resolution although the value of the roughness parameters will all increase. The terrain map can be used to separate the resolvably rougher areas, Units III, IV, V, and VI, from those that are relatively featureless. Unit II, the apparently smooth terrain covered by ray material, can be eliminated from further consideration on the basis of visual

studies that indicate a high degree of roughness at the limit of telescopic resolution. Since roughness is additive, these areas have a very low probability of containing any extensive smooth terrain at the one to ten meter scale. This leaves only Unit I for consideration with regard to possible landing areas for both unmanned and manned spacecraft. The areal extent of this Unit is about 20 percent of the equatorial belt, thus effectively narrowing the search area of unmanned spacecraft. Detailed studies by means of systematic traverses in the central part of the equatorial belt have further reduced the areal extent of this statistically favorable unit.

Integrated Slope Distribution Map

Plates 2, 3, 4, 5, and 6 represent a statistical treatment of the slope values derived from systematic photometric traverses on two high resolution photographic plates in the central part of the moon (Mt. Wilson, P124 and P192). This approach was decided upon in lieu of attempting to make contour maps because of the lack of any slope information in the north-south direction. The positions of the photometric traverses on the original plate have been transferred by inspection to a lunar grid derived from the 1:1, 000, 000 LAC Series of the Aeronautical Chart and Information Center, and the slope measurements plotted and categorized into four intervals. The intervals were selected for the purpose of outlining in the most effective way possible those areas that are resolvably smoothest. A conservative estimate of the limit of accuracy of the method in regions of low slope is about one third of a degree. Therefore, the

smoothest category shown (0 to 0. 7 degrees) represents areas which in no case exhibit slopes of more than one degree and in the majority of cases represent slopes considerably less.

The areal extent of each categorized slope element was extended one half the distance in the north-south and the east-west directions to the next measurement. The type of map developed is useful in portraying areal distribution patterns of absolute slope values independent of the rate of change of these values as is usually portrayed by a contour map. The objective of these maps is not to depict topography which is best done by the conventional contour map, but rather to show the distribution pattern of the measured slope components. This integrated slope distribution map so derived can be used effectively in such operations as determining the probability of landing on reasonably smooth terrain given a landing circle of any designated size.

These maps show that the smoothest regionally extensive area in the central part of the equatorial belt is within the northern extension of Mare Nubium, to the east of crater Palisa (Plate 6). A number of smaller favorable areas lie between eight and 14 degrees west longitude, and between two and eight degrees north latitude as seen on Plate 5. Plates 3 and 4, generally in the highlands, show few areas with consistently low slope readings. Only one area of any extent can be interpreted as being favorable, i. e., the area near the crater Réaumur.

Visual Studies

Of the eight areas selected for visual studies, poor "seeing" conditions precluded, for the most part, effective work, at Lick Observatory, California, and at Kitt Peak Observatory, Arizona. One observer, however, did experience good conditions when observing the Flamsteed area, 0°-6°S, 42°-46°W (Figure 10) with the 36" refracting telescope at Lick Observatory. Under conditions of excellent "seeing" one can visually resolve at this telescope craterlets as small as one quarter of a mile in diameter and linear clefts as small as 25 yards in width. It is estimated that most of the small shadowed areas observed in this study range in size from several hundred yards to a thousand yards. The work here, however, was limited to a detailed qualitative study of the relative roughness at low angles of illumination. The area was divided into four units arranged in order of relative observable roughness. The degree of roughness was determined by the incidence of the smallest resolvable shadows close to the terminator. The regions showing the largest percent of shadowed terrain alternating with small illuminated areas were judged to be the roughest and those showing the least variation in illumination were considered the smoothest.

The area with the least resolvable roughness corresponds to the darkest part of the maria in this area of the moon. The darker maria generally exhibit the lowest photometric slope frequency distributions throughout the equatorial belt. The general relationship that appears to exist between resolvable roughness and the

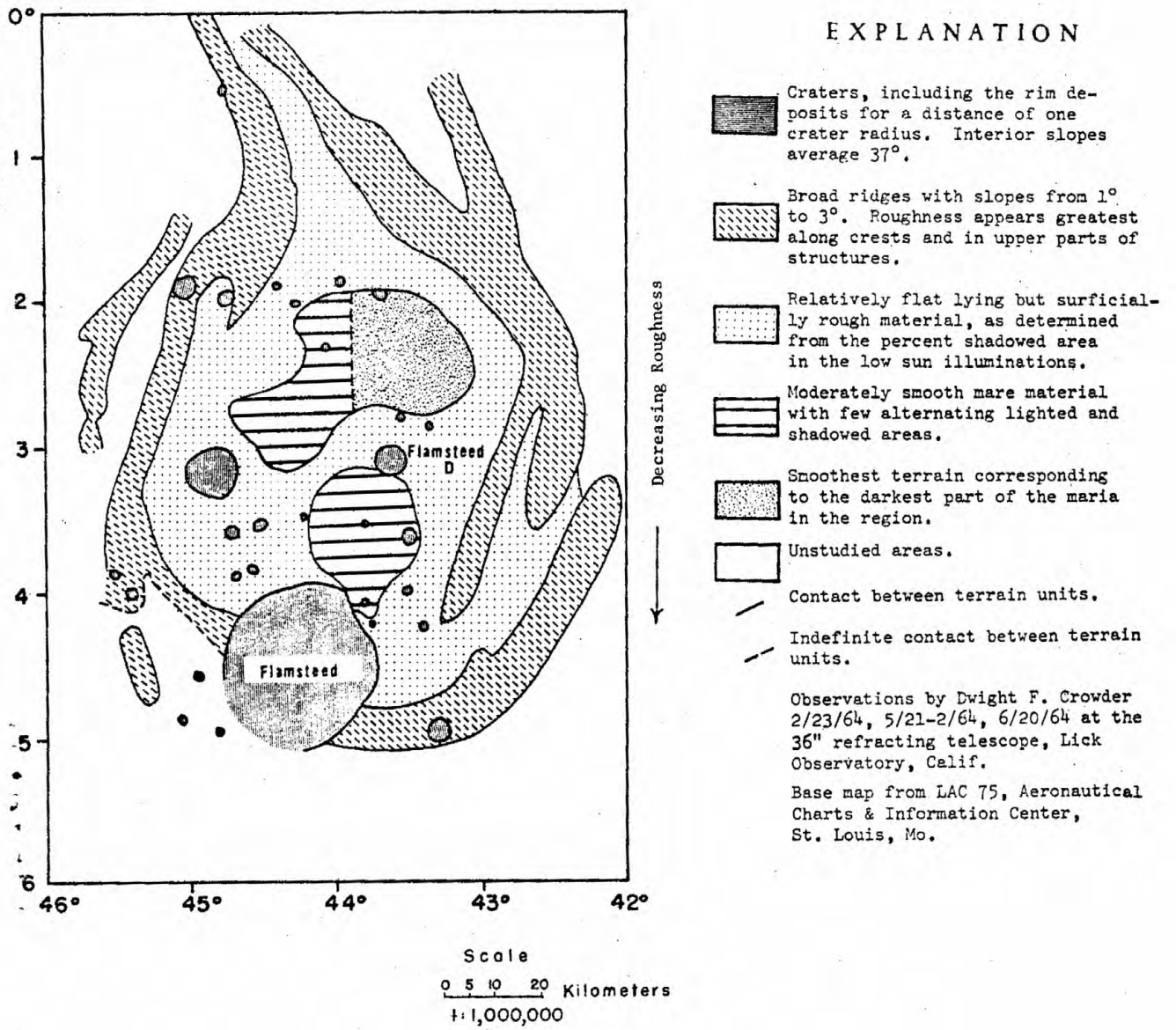

Figure 10. Terrain map of the Flamsteed area derived by visual telescopic study at the Lick 36" refractor.

albedo of the maria may be helpful in making the final selection of areas for further study by unmanned spacecraft.

Terrestrial Slope Frequency Distribution Studies

In order to develop an appreciation of the relationship between surface roughness and the scale or resolution at which it is measured, studies of selected terrestrial areas were undertaken. These studies also provide information on the problem of extrapolating roughness to larger scales below the limit of resolution.

Three areas were selected for initial study. They are the Sierra Nevada Region, California; the San Juan Mountain Region, Colorado; and the Mogollon Rim Region, Arizona. All are characterized by very rough topography and by an essentially random orientation of slopes as evidenced by a predominantly dendritic drainage pattern. In each area a series of three profiles was prepared and alternate slope segments measured. The sample intervals used were one kilometer at the 1:1, 000, 000 scale; 0. 25 kilometers at the 1:250, 000 scale, and 0. 06 kilometers at the 1:62, 500 scale. Alternate slope segments were measured in order to simulate as closely as possible the sampling technique used in the photometric method. The data was arranged in the form of cumulative slope frequency curves to provide a measure of relative roughness (Figure 11). The median slope values at the 1:1, 000, 000 scale range from 2. 5 degrees to 4. 0 degrees, approximately equivalent to the average values of lunar terrain units V and VI at the same scale.

At a scale of 1:250, 000, the value of median slope has

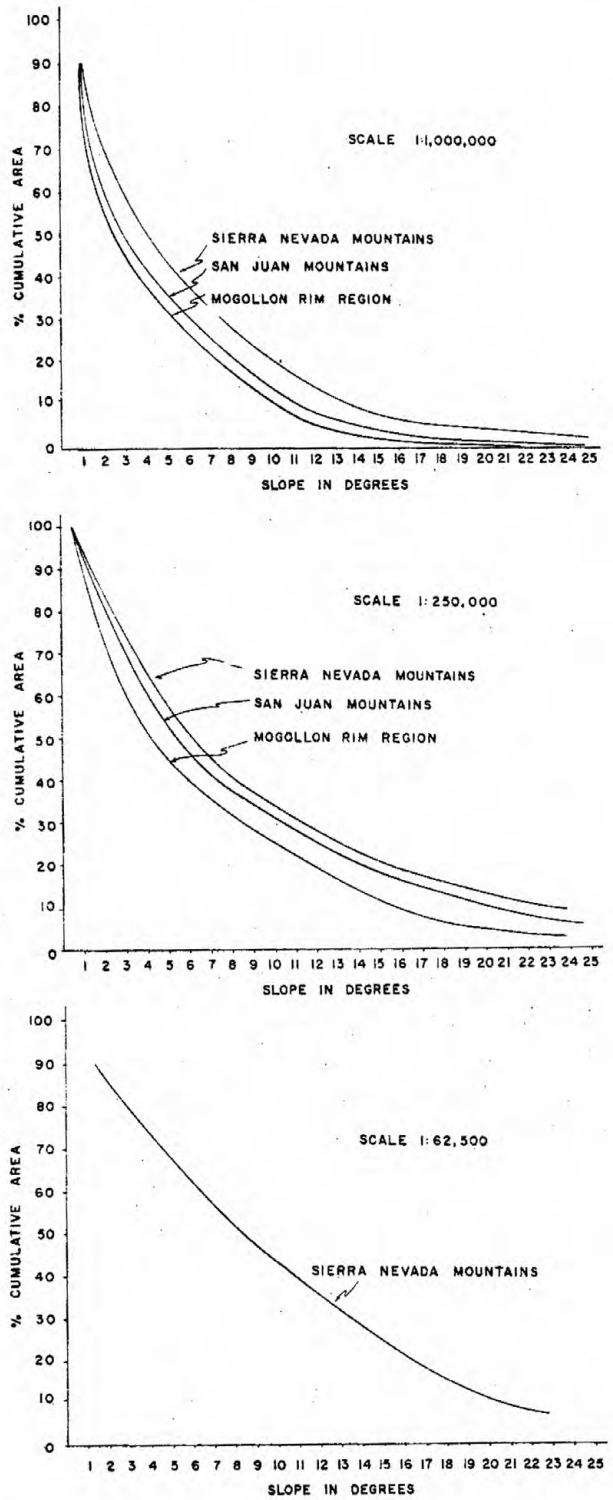

Figure 11. Terrestrial slope frequency distribution curves for rough terrain measured at varying scales.

increased considerably along with the dispersion of the 10-90 percentile range. Sampling the Sierra Nevada area at 1:62, 500, demonstrated that the roughness increased further with increasing resolution.

These measurements indicate that median slope values of 2. 5 degrees to four degrees at the 1:1, 000, 000 scale are representative of very rough terrain. These values are comparable to those obtained for the roughest lunar terrain within the equatorial belt; this means that although the geometry of each is quite different at the one kilometer scale the slope frequency distribution for lunar mountainous terrain is very similar to that of the very rough terrestrial terrain. Figure 12 shows two oblique aerial views of the Mogollon Rim area, Arizona, an area with a 2. 5 degree median slope value at the one kilometer scale. The photograph (average foreground resolution ten feet) clearly indicates that terrain with median slope values on the order of two degrees or above would have a very low probability of containing safe spacecraft landing areas.

In order to determine the relationship between scale or resolution and median slope, this value was plotted as a function of the slope length for the different map scales studied (Figure 13). It is apparent that the median slope value for the San Juan area and the Sierra Nevada area increases as a simple power function as the resolution or scale increases. The slope of this curve indicates the rate at which the roughness increases for the particular region. This value might prove useful in future terrain quantification studies. The rate of increase

Plate A. Oblique aerial view of the Mogollon Rim Region, Arizona, near Mazatzal Mountains (altitude 12, 000 ft., 8:00 am, 1964). Average foreground resolution is one meter.

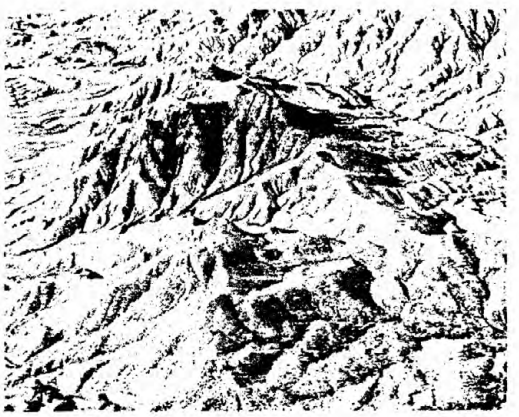

Plate B. Oblique aerial view of the Mogollon Rim Region, Arizona, near Mazatzal Mountains (altitude 10, 000 ft., 8:15 am, 1964). Average foreground resolution is 0. 5 meters.

Figure 12. Aerial photographs showing terrain with same statistical slope distribution at the one kilometer scale as the lunar uplands (terrae).

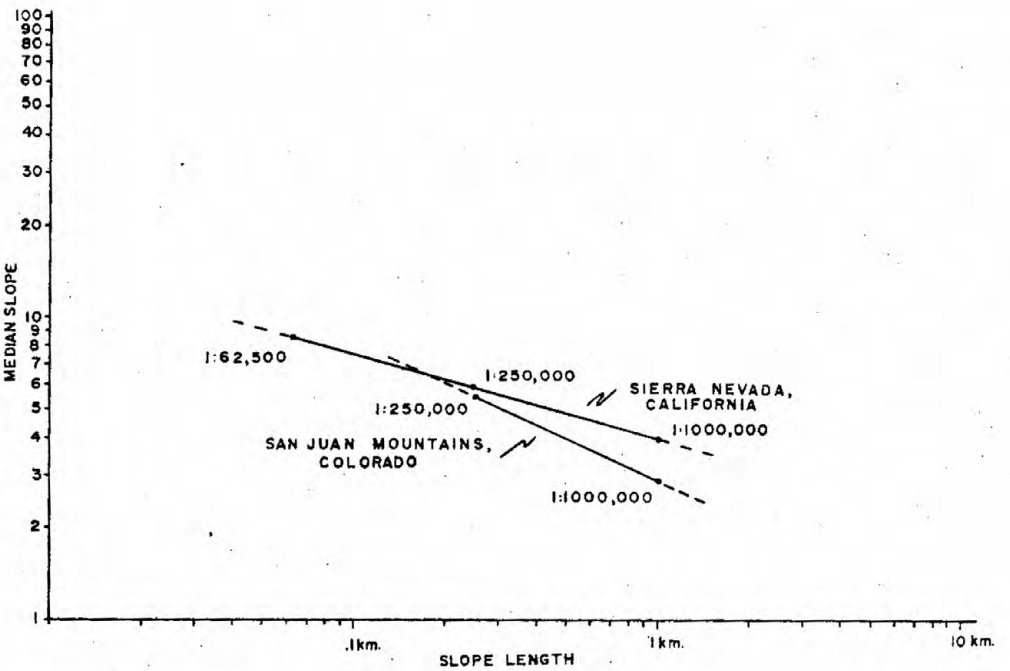

Figure 13. Median slope values for two rough terrestrial areas plotted as a function of slope length.

of the median slope may vary for a particular terrain, and the curve may flatten out over a wide range so that the median will not increase significantly with increasing resolution. If the area measured is kept the same, however, the median slope value can never decrease with increasing resolution, and the roughness below the limit of resolution is always additive to that above it.

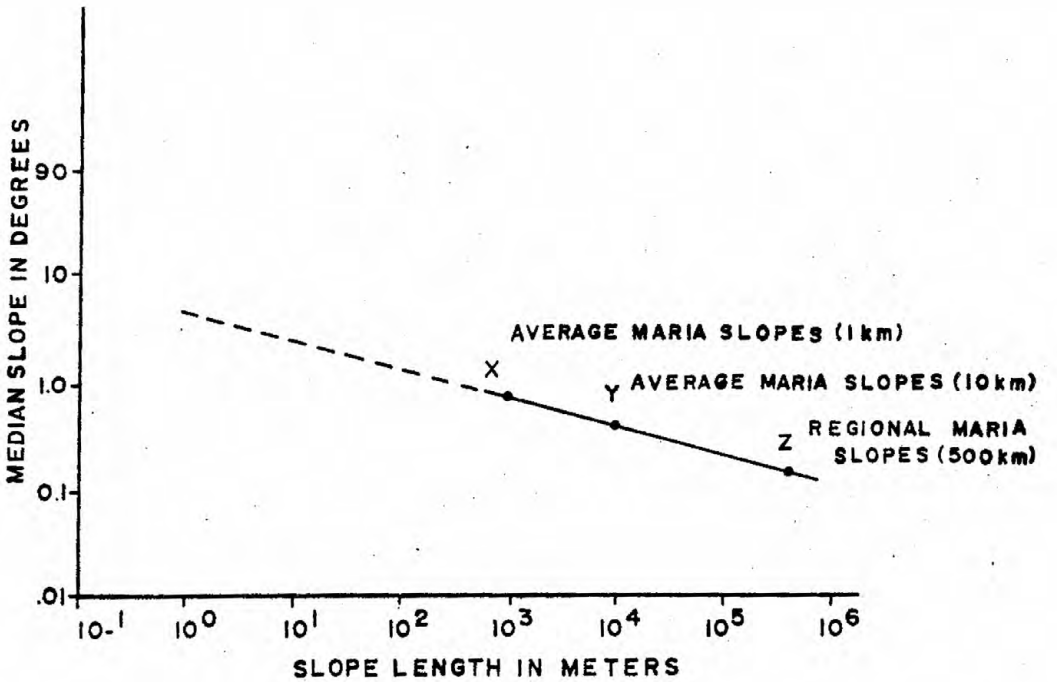

Figure 14. Median slopes plotted as a function of slope length for the lunar maria.

Extrapolation of Roughness Below the Limit of Resolution

The terrestrial studies of rough terrain indicate that the rate of change of the median slope value does remain constant through the one kilometer to 0. 1 kilometer range, and that it may be possible to extrapolate median slope values from low to high resolution if part of the curve is known. The same extrapolation can be performed in this range for different lunar terrain types in order to estimate the statistical distribution of slopes below the limit of telescopic resolution. It is believed that the

References

Amdursky, M. E., Marsh, E. A., and Graboske, H. C., Jr., 1964, LRV Optical Studies Interim Progress Report, March, 1964: The Bendix Corporation, Ann Arbor, Michigan, 30 p.

Chayes, Felix, 1956, Petrographic Modal Analysis: New York, John Wiley and Sons, Inc., 113 p.

Dale, E. D., 1962, The application of the van Diggelen method of slope analysis to lunar domes and wrinkle ridges: Thesis University of Manchester, England, 46 p.

Diggelen, J. van, 1951, A photometric investigation of the slopes and the heights of the ranges of hills in the maria of the moon: Astron. Inst. Netherlands Bull., v. 11, no. 423, p. 283-289.

Hawkins, J. K., and Munsey, C. J , 1963, Automatic photo reading: Photogrammetric Engineering, v. 29, no. 4, p. 632-640.

Pohn, Howard, Murray, Bruce C., and Brown, Harrison, 1962, New applications of lunar shadow studies: Publ. Astron. Soc. Pacific, v. 74, no. 437, p. 93-105.

Wilhelms, D. E., 1963, A photometric technique for measurement of lunar slopes: U. S. Geol. Survey, Astrogeologic Studies annual progress report, Aug 25, 1962 to Jul 1, 1963, part D, p. 1-12.